On the "bridge hill" of the violin

J. Woodhouse
Cambridge University Engineering Department,
Trumpington St, Cambridge CB2 1PZ, U.K.

jw12@eng.cam.ac.uk

Summary

Many excellent violins show a broad peak of response in the vicinity of 2.5 kHz, a feature which has been called the "bridge hill". It is demonstrated using simplified theoretical models that this feature arises from a combination of an in-plane resonance of the bridge and an averaged version of the response of the violin body at the bridge-foot positions. Using a technique from statistical vibration analysis, it is possible to extract the "skeleton" of the bridge hill in a very clear form. Parameter studies are then presented which reveal how the bridge hill is affected, in some cases with great sensitivity, by the properties of the bridge and body. The results seem to account for behaviour seen in earlier experimental studies, and they have direct relevance to violin makers for guiding the adjustment of bridges to achieve desired tonal quality.

PACS No. 43.75.De

1. Introduction

The characteristic high bridge of the violin and cello, and indeed of most bowed-string instruments, presumably developed initially for ergonomic reasons. In order to provide the range of angles needed to bow each string individually, the strings must be raised clear of the instrument body. Also, the high bridge plays an essential role in "rotating" the transverse force from the vibrating string into normal forces applied to the instrument body through the bridge feet, which can then excite bending vibration of the body [1]. Compared to the low, robust bridges of the piano or guitar, the violin bridge may seem to be a necessary evil: it is fragile and requires regular attention to keep it straight and properly fitted. However, research of recent years shows that this type of bridge has provided, perhaps somewhat fortuitously, a crucial means for adjustment of the string-to-body impedance characteristics which has allowed the violin family to acquire its familiar loudness and tonal colouration.

The oscillating force provided by the vibrating string can only excite vibration of the instrument body by first passing through the bridge. The bridge thus acts as a filter, and it is no surprise that the material properties and geometric configuration of the bridge can have a significant influence on the sound of an instrument. The first systematic study of the transmission properties of the violin bridge was made by Reinicke and Cremer [1,2]. They showed that a normal violin bridge has internal resonances within the frequency range of interest for the sound of the instrument, so that the filtering effect of the bridge has very significant variation with frequency. The lowest bridge resonance is usually found around 3 kHz when the bridge feet are held rigidly (for example in a vice), and the motion consists of side-to-side rocking of the top portion of the bridge as sketched in Fig. 1.

Since the work of Reinicke and Cremer, several experimental studies have been carried out which relate to the influence of this lowest bridge resonance. First, measurements have been made by Dünnwald [3] and Jansson [4,5] of the frequency response of a wide variety of violins. Both authors found that violins of high market value showed a strong tendency to exhibit a broad peak of response in the vicinity of 2–3 kHz, in a feature originally named the "bridge hill" by Jansson. The name was given because he, and indeed Cremer [1], attributed this feature to the filtering effect of the lowest bridge resonance just described. A typical

example is shown in Fig. 2: the plot shows the input admittance (velocity response to unit force amplitude) in the direction of bowing, measured at the string position on a violin bridge using a method similar to that described by Jansson [4]. The characteristics of the bridge hill are seen clearly in Fig. 2: a rise in amplitude around the peak frequency of the "hill", followed by a steady drop in amplitude at higher frequencies, and over the same frequency range a downward trend in phase towards –90°.

The second relevant set of experimental studies is the extensive series reported by Jansson and co-workers [6,7,8] in which various structural modifications were made to the bridge and/or the top plate of the violin, and the effect on the input admittance measured. These studies have shown that the appearance of a "bridge hill", and its frequency, are not determined by the bridge structure alone. In particular, they reveal that the feature can sometimes still be seen when the standard bridge is replaced by a "plate bridge" with no cut-outs, so that the vibration mode shown in Fig. 1 is no longer possible. Jansson's measurements also showed a significant influence arising from the spacing of the bridge feet [7] and the stiffness/mass of the top plate in the vicinity of the bridge [6]. These results led Jansson to become less satisfied by the name "bridge hill", and he has advocated "bridge-body hill", or just "hill" [6]. However, it will be argued that the bridge is still the central defining element in the phenomenon, and the original name "bridge hill" will be retained here.

The fact that the frequency of a bridge resonance will be significantly affected by the coupling to the violin body was already stressed by Reinicke and Cremer. The results of Jansson have fleshed this idea out with empirical data. The task of this paper is to explain the pattern of behaviour and show how the frequency, height and shape of the bridge hill are influenced by the constructional parameters of the bridge and violin. A first step has been taken by Beldie [9], who has shown that a reasonable fit to Jansson's results can be obtained if the behaviour of the body beneath the bridge feet is approximated by simple springs. In particular, his idea explains why there can still be a "bridge hill" with Jansson's plate bridge without cut-outs: the mode consists of side-to-side rocking motion of the entire bridge, with a restoring force provided by the "springs" under the feet. However, Beldie gave no explanation for what determines the stiffness of these "effective springs", and more importantly, no-one appears to have addressed the question of what determines the height and bandwidth of the bridge hill.

The approach here will be to explore the bridge hill using simplified theoretical models which are "violin-like" but which remain simple enough to analyse without needing elaborate finite-element calculations This simplification is convenient, but more importantly it can be combined with recent developments in vibration theory to allow a calculation of the underlying "skeleton" of the frequency response curve, not readily accessible from a detailed prediction such as a finite-element model. Once it has been shown that the skeleton calculation is reliable, this approach will allow attention to be focused on the parameters which influence the "hill" without the distracting details of the individual body resonance peaks. All the general features reported by Jansson can be demonstrated with these simplified models. One particular conclusion of this study will be that the bridge hill observed by Dünnwald [3] and Jansson [4,5] in many valuable instruments is probably not primarily a property of the instruments as such, but a result of the fact that more care and attention has been devoted to the fitting of appropriate bridges to these instruments. This suggestion is in keeping with the experience of experts in violin set-up, who attribute great importance to bridge adjustment.

2. Modelling the bridge and body

The amplitude and phase characteristics seen in Fig. 2 are precisely what would be expected when a multi-modal system (the violin body) is driven through an intermediate system exhibiting a resonance. The simplest example is shown schematically in Fig. 3. A force $Fe^{i\omega t}$ is applied to a mass m, which in turn drives a system with input admittance $Y_v(\omega)$

through a spring of stiffness k. (The subscript "v" indicates "violin".) It is straightforward to show that the input admittance of the combined system is

$$Y_b(\omega) = \frac{kY_v + i\omega}{k - m\omega^2 + i\omega k m Y_v} \tag{1}$$

where the subscript "b" indicates "bridge".

For a clear demonstration that this equation predicts behaviour similar to the observed bridge hill, it is convenient to use a very idealised system $Y_v(\omega)$: assume regularly spaced resonances, all with the same amplitude and damping factor. Then Fig. 4a shows a plot of $Y_v(\omega)$, and Fig. 4b shows a typical plot of $Y_b(\omega)$. Parameter values are given in the caption. The dashed lines will be discussed in Section 3, and should be ignored for the moment. It is immediately clear that Fig. 4b shows similarities to Fig. 2: the regular peaks of $Y_v(\omega)$ have been modulated by a "hill" followed by a steady amplitude decline, while the phase plot shows a downward trend towards –90°. (Note that the phase of the input admittance cannot go negative beyond –90°, because the system is assumed to be dissipative at all frequencies, rather than containing any energy source. This requirement is often used as a check on the phase accuracy of measurements.)

This simple formulation is not quite sufficient to capture the behaviour of a violin bridge. It is necessary to take into account that the bridge contacts the violin body at two points rather than one. The natural model is the one put forward by Reinicke and Cremer [1,2], equivalent to that sketched in Fig. 5. The portion of the bridge below the "waist" can be regarded as a rigid body, coupled via a torsion spring to a mass-loaded rigid link representing the rotational inertia of the upper part of the bridge. The vibrational force from the string drives this upper mass transversely. This bridge model is parameterised by the foot spacing d, the length a of the rotating link, the mass m and the torsional spring stiffness K. The resonant frequency of the bridge with its feet rigidly clamped is then

$$\Omega_b = \frac{1}{a}\sqrt{\frac{K}{m}} \ . \tag{2}$$

The admittance $Y_b(\omega)$ at the "string notch", in other words at the mass m, is now to be calculated in terms of these parameters, together with the 2×2 admittance matrix which describes the properties of the violin body at the two foot positions. A useful intermediate stage is to calculate the "rotational admittance" governing the motion of the lower part of the bridge: this admittance $R(\omega)$ is defined as the angular velocity of the bridge base when a moment is applied to it of unit magnitude, oscillating sinusoidally at frequency ω. Assuming that the mass of the bridge base is small enough to be neglected, it is easy to show that

$$R = \frac{Y_{11} + Y_{22} - 2Y_{12}}{d^2} \tag{3}$$

where $Y_{jk}(\omega)$ denotes the velocity response of the violin body at the position of bridge foot k to a harmonic force of unit amplitude applied at bridge foot j.

This admittance can also be written in terms of the modes of the violin body. The body admittance matrix is given by the standard formula (see for example [10])

$$Y_{jk}(\omega) = \sum_n \frac{i\omega u_n(x_j, y_j) u_n(x_k, y_k)}{\left(\omega_n^2 + 2i\omega\omega_n\zeta_n - \omega^2\right)} \tag{4}$$

where the *n*th mode of vibration of the body in the absence of the bridge has mode shape $u_n(x,y)$ at position (x,y), natural frequency ω_n and modal damping factor ζ_n (or corresponding modal Q-factor $Q_n = 1/2\zeta_n$). The positions of the two bridge feet have coordinates $(x_1, y_1), (x_2, y_2)$. The mode shapes are assumed to be normalised in the usual way with respect to the system mass matrix or kinetic energy function [10]. Substituting in eq. (3) yields

$$R(\omega) = \frac{i\omega}{d^2} \sum_n \frac{\left[u_n(x_1, y_1) - u_n(x_2, y_2)\right]^2}{\left(\omega_n^2 + 2i\omega\omega_n\zeta_n - \omega^2\right)} \ . \tag{5}$$

In the limit $d \to 0$ this expression tends towards the point moment admittance of the plate, involving the squared spatial derivative of the mode shapes.

Imposing moment balance around the torsion spring in the bridge model now yields an expression for the input admittance at the top of the bridge which is analogous to eq. (1):

$$Y_b(\omega) = \frac{(KR + i\omega)a^2}{K - ma^2\omega^2 + i\omega Kma^2 R} \ . \tag{6}$$

The similarity is sufficiently close that "bridge hill" behaviour like that shown in Fig. 4 can confidently be expected. To explore the consequences requires a more realistic choice of model for the "violin body" than that used before, since to evaluate R requires mode shape information.

There is only one vibration problem involving a two-dimensional bending plate which has a simple closed-form solution, and it is natural to use this as a first approximation. This system is a rectangular plate with hinged boundary conditions all around. If the plate has plan dimensions $L_1 \times L_2$, thickness h and density ρ, then the normalised mode shapes ready for substitution into eqs. (4) or (5) are

$$u_{nm} = \frac{2}{\sqrt{L_1 L_2 h \rho}} \sin\frac{n\pi x}{L_1} \sin\frac{n\pi y}{L_2} \tag{7}$$

where the term under the square root is simply the total mass of the plate, and x and y are Cartesian coordinates in the plane of the plate, measured from one corner. The corresponding natural frequencies satisfy

$$\omega_{nm}^2 = \frac{h^2}{\rho}\left[D_1\left(\frac{n\pi}{L_1}\right)^4 + D_3\left(\frac{m\pi}{L_2}\right)^4 + \left(D_2 + D_4\right)\left(\frac{n\pi}{L_1}\right)^2\left(\frac{m\pi}{L_2}\right)^2 \right] \tag{8}$$

where $D_1 - D_4$ are the elastic constants appropriate to a plate of orthotropic symmetry, as discussed in detail by McIntyre and Woodhouse [11]. Suitable numerical values for these elastic constants for "instrument-like" plates of spruce or maple, together with other numerical values used in the "violin" models here, are given in Table 1.

Using this model, the "rotational admittance" R is plotted in Fig. 6 and the input admittance at the bridge top is shown in Fig. 7. The dashed lines in these plots will be explained in the next section. Figure 6 shows no very strong trend with frequency, somewhat similar to Fig. 4a, while Fig. 7 shows a clear bridge hill. Also, the absolute level of the admittance in Fig. 7 is similar to that seen in Fig. 2, confirming that this simple model has broadly violin-like behaviour. The aspect of this model which is most obviously unrealistic is not immediately apparent from these plots. Because the "bridge" has been placed symmetrically with respect to the mid-line of the plate, many of the plate modes do not contribute to R. These modes have motion that is symmetrical at the two bridge feet so that, from eq. (5), their contribution to R is zero. In a real violin, the presence of the bass bar and soundpost destroy the symmetry of the structure, so that potentially all modes could contribute to R.

It is not easy to incorporate a bass bar into the idealised model used here, but a representation of the soundpost is quite simple to achieve. The model can be extended to include two rectangular plates, representing the top and back of the violin. Both will have the same plan geometry, and will have hinged boundaries along all edges. The two plates can then be coupled together at a chosen point by a massless, rigid link representing the soundpost. Such point-coupled systems are easily modelled using appropriate combinations of the admittances. If the only requirement were the driving-point admittance Y_{coup} of the coupled plates at the "soundpost" position, it would be given simply by

$$\frac{1}{Y_{coup}} = \frac{1}{Y_1} + \frac{1}{Y_2} \tag{9}$$

where Y_1, Y_2 are the input admittances of the two uncoupled systems at the same position. This familiar formula expresses the fact that the displacements of the two coupled systems are the same at the coupling point, while the total applied force is the sum of the forces applied to the two separate subsystems.

A slightly more complicated version of this argument is needed in order to give the admittances $Y_{jk}(\omega)$ relating to the positions of the bridge feet, neither of which is exactly at the soundpost position. If the soundpost has coordinates (x_3, y_3) on both top and back plates, then the required admittances can be obtained from the formula

$$\begin{bmatrix} Y_{11}^{coup} & Y_{12}^{coup} & Y_{13}^{coup} \\ Y_{21}^{coup} & Y_{22}^{coup} & Y_{23}^{coup} \\ Y_{31}^{coup} & Y_{32}^{coup} & Y_{33}^{coup} \end{bmatrix}^{-1} = \begin{bmatrix} Y_{11}^{uncoup} & Y_{12}^{uncoup} & Y_{13}^{uncoup} \\ Y_{21}^{uncoup} & Y_{22}^{uncoup} & Y_{23}^{uncoup} \\ Y_{31}^{uncoup} & Y_{32}^{uncoup} & Y_{33}^{uncoup} \end{bmatrix}^{-1} + \begin{bmatrix} 0 & 0 & 0 \\ 0 & 0 & 0 \\ 0 & 0 & 1/Y_{33}^{back} \end{bmatrix} \tag{10}$$

where the superscripts "coup" and "uncoup" label the top-plate admittances from eq. (4) in the coupled and uncoupled states respectively, in matrices relating to the three positions $(x_1, y_1), (x_2, y_2), (x_3, y_3)$. Y_{33}^{back} is the input admittance at the soundpost position on the uncoupled back plate. Equation (10) embodies the same physical argument as above, stating that an impedance $1/Y_{33}^{back}$ has been added to the top plate at the soundpost position, while nothing has been added at the positions of the bridge feet.

Using this extended model with the numerical values given in Table 1, the rotational admittance is now as shown in Fig. 8 and the input admittance at the bridge top is as shown in Fig. 9. These two figures are directly comparable with Figs. 6 and 7 respectively. Again, the dashed lines in the plots will be discussed in the next section. Many more peaks are seen than in the plots from the simpler model, both because the symmetry has been broken and because

the back plate has introduced additional resonances of its own. The trends are generally similar, with a clear bridge hill seen in Fig. 9. Notice that the hill is rather higher and narrower than in Fig. 7. This extended model will be used to investigate the influence on the bridge hill of various parameters relating to the bridge and to the "violin body".

It is interesting to compare Fig. 9 with the measured admittance in Fig. 2. This reveals that the general levels are quite similar except near the hill, which is a little too prominent in this particular simulation. However, it will be seen in section 4 that the parameter values of the bridge model could readily be altered to achieve a closer match of the hill. The other obvious difference between Figs. 2 and 9 is that the flat-plate "violin" has a higher density of resonances at low frequencies than the real violin. The reason for this probably lies mainly in the arched plates of the real violin: curved shells such as cylinders have low modal density below the "ring frequency" [12], but at higher frequencies they tend towards the same modal density as a flat plate of the same area. The ring frequency in Hz is given by $c / 2\pi R$, where R is the radius of the cylinder and c is the compressional wave speed. It is not influenced by the thickness of the shell. There is no single "ring frequency" for the complex geometry of a violin plate, but simple estimates based on typical axial or transverse radii of curvature of a violin top, and the corresponding wave speeds of spruce, yield values of the order of 1–2 kHz. At frequencies of relevance to the bridge hill, the flat-plate model should have similar modal density to the real violin. The model seems good enough that one might hope to obtain plausible bridge-hill shapes with numerical values of bridge parameters close to those measured from real bridges.

3. The response skeleton

Before looking at parameter studies, though, it is desirable to find a way to focus on the underlying hill without the distracting details of the individual body modes. This can be done readily for this simple model, by using an approach known in different guises as "Skudrzyk's mean value method" [13] or "fuzzy structure theory" [14]. Skudrzyk's argument is the most direct for the present purpose. The key insight is that, from eq. (4), the height of an isolated modal peak is proportional to $1 / \zeta_n$, while the level at an antiresonance dip is proportional to ζ_n. It follows that the mean level of a logarithmic plot follows the geometric mean of these two, and is thus independent of damping. If the damping were increased, the peaks and dips would blur out and all admittance curves would tend towards smooth "skeleton" curves representing the logarithmic mean of the original curves.

There is a physically appealing way to visualise the effect of increasing the damping. When a force is applied at a point on the structure, it generates a "direct field" consisting of outward-travelling waves. In time these will reflect from the various boundaries and return. Modal peaks will occur at frequencies where the reflections combine in phase-coherent ways. Antiresonances occur when the sum of reflected waves systematically cancels the original direct field. But at an "average" frequency, where neither of these coherent phase effects occurs, the reflected waves from the various boundaries tend to arrive in random phases and to cancel each other out, leaving the direct field to dominate the response. If damping is increased, the influence of reflections decreases. In the limit of high damping, the desired "skeleton" of the admittance is given by the direct field alone.

The effect is thus the same as if the plate boundaries had been pushed further away until the system becomes *infinitely large*. This gives a simple recipe to find skeleton curves for the models discussed above: the rectangular top and back plates are replaced by infinite plates with the same material properties and thicknesses. The vibration of a point-driven infinite plate has a simple closed-form solution. For a plate of isotropic material of density ρ, Young's modulus E, Poisson's ratio ν and thickness h the driving-point admittance is

$$Y_\infty(\omega,0) = \frac{1}{4h^2}\sqrt{\frac{3(1-\nu^2)}{E\rho}}\ , \tag{11}$$

which represents a pure resistance: it is real and independent of frequency. For response at a point a distance r from the driven point, the transfer admittance is

$$Y_\infty(\omega,r) = \frac{1}{4h^2}\sqrt{\frac{3(1-\nu^2)}{E\rho}}\left[H_0^{(2)}(kr) - H_0^{(2)}(-ikr)\right] \tag{12}$$

where the wavenumber k is given by

$$k^4 = \frac{12\rho(1-\nu^2)\omega^2}{Eh^2} \tag{13}$$

and $H_0^{(2)}$ is the Hankel function of the second kind of order zero [15].

For a plate of orthotropic material like wood the behaviour is somewhat more complicated, but a standard approximation is sufficiently good for the present purpose. If it is assumed that

$$D_2 + D_4 = 2\sqrt{D_1 D_3} \tag{14}$$

then the plate is equivalent to an isotropic one provided distance x "along the grain" is scaled relative to distance y "across the grain" according to

$$\hat{x} = x\left(D_3 / D_1\right)^{1/4}. \tag{15}$$

The equivalent result to eq. (12) is then

$$Y_\infty(\omega) = \frac{1}{8h^2\sqrt{\rho\sqrt{D_1 D_3}}}\left[H_0^{(2)}(kr) - H_0^{(2)}(-ikr)\right] \tag{16}$$

where

$$k^4 = \frac{\rho\omega^2}{D_3 h^2} \tag{17}$$

and r is calculated using $(\hat{x}, y)$. To illustrate the behaviour predicted by eq. (16), Fig. 10 shows the real and imaginary parts of Y_∞ for the parameters of the spruce plate used in the models in the previous section, and a value of r equal to the bridge-foot spacing assumed there.

The calculations of the previous section can be readily repeated using these infinite-plate admittances in place of the finite-plate results used before: in particular, eq. (10) can still be used to give a model which allows for the soundpost, but treats both the top and back plates as infinite in extent. The results are shown as dashed lines in Figs. 4, 6–9. It is clear that these dashed lines do indeed follow accurately the mean trend of the logarithmic amplitude and the phase, and also that they reveal the form of the bridge hill in Figs. 4b, 7 and 9. The skeleton curves based on this infinite-plate modelling have been found to show similar accuracy over a

wide range of parameter values. It seems clear that, to study the bridge hill, it will be sufficient to study these simple skeleton curves.

Some conclusions can be drawn immediately. The skeleton of the input admittance at the bridge is given by eq. (6) with R replaced by the "skeleton" value R_∞. It is plausible, and confirmed by the dashed lines in Figs. 6 and 8, that this value varies only slowly with frequency. Substituting a constant value appropriate to the general vicinity of the bridge hill, eq. (6) shows that the form of the hill is determined by complex poles which are the roots of

$$\omega^2 - i\omega R_\infty K - \Omega_b^2 = 0. \tag{18}$$

If R_∞ is real, this takes the familiar form of a damped harmonic oscillator which represents the bridge resonance damped by radiation through the feet into the infinite plate system. The effective damping factor ζ_b of this "hill oscillator" can be written in several equivalent forms:

$$\zeta_b = R_\infty K / 2\Omega_b = R_\infty m a^2 \Omega_b / 2 = R_\infty a\sqrt{Km} / 2. \tag{19}$$

If ζ_b is small the bridge hill will appear as a tall, narrow peak close to the clamped bridge frequency Ω_b. As ζ_b increases, the bridge hill moves down somewhat in frequency and the peak becomes broader and lower. If ζ_b reaches unity the bridge hill becomes critically damped so that it ceases to be visible as a "hill" and simply becomes a low-pass filter. Equation (19) thus shows how the various model parameters combine to determine the height and bandwidth of the bridge hill, an aspect which has not been much discussed in the literature of the subject.

If R_∞ is complex the interpretation of eq. (18) is a little less obvious. An estimate of the damping factor of the hill can probably be obtained from eq. (19) by replacing R_∞ with $\mathrm{Re}(R_\infty)$, but the imaginary part of R_∞ will contribute a reactive effect which will shift the frequency of the hill away from the clamped frequency Ω_b. This is the physical origin of the effect observed by Jansson [6,8], and idealised by Beldie in terms of effective springs beneath the bridge feet [9]. Indeed, it is simple to obtain from eq. (18) an estimate of the hill frequency when the flexible bridge is replaced with a rigid "plate bridge" as in Jansson's experiments [6]. Rewriting eq. (18) in the form

$$\omega^2 - i\omega R_\infty K - K / (ma^2) = 0 \tag{20}$$

then allowing $K \to \infty$, it is clear that the first term of eq. (20) becomes negligible in the frequency range of interest, and the effective pole frequency is given by the other two terms as

$$\omega \approx i / \left(ma^2 R_\infty\right). \tag{21}$$

This expression clearly shows the hill frequency arising under these limiting conditions from a balance between (rotational) stiffness provided by the violin body, and inertia provided by the bridge.

To look a little more closely at the behaviour when R_∞ is complex, the flat-plate model can be used to suggest appropriate numerical values to explore. Figure 11 shows the real and imaginary parts of R_∞ corresponding to Fig. 8. For a bridge hill in the vicinity of 2.5 kHz, it seems reasonable to take $\mathrm{Re}(R_\infty) = 100$ rad m^{-1}s^{-1}N^{-1} and to explore a range of $\mathrm{Im}(R_\infty)$ of the same order of magnitude. Figure 12 shows the resulting variation of hill frequency and

loss factor, obtained by solving eq. (18) exactly. The frequency can be raised or lowered relative to the clamped frequency (3 kHz here), depending on the sign of $\mathrm{Im}(R_\infty)$: there seems to be no physical reason why it should necessarily be positive (and hence "spring-like"). The loss factor turns out to be influenced very little by $\mathrm{Im}(R_\infty)$: it remains close to the value given by eq. (19) with R_∞ replaced by $\mathrm{Re}(R_\infty)$, shown as the dashed line.

4. Parameter studies

4.1. Parameters of the bridge

The flat-plate model does not by any means represent all relevant features of the violin body, but it contains enough detail that considerable insight of a semi-quantitative nature can be gained by varying the parameters of the model. Sets of "skeleton" curves will be shown to illustrate how the bridge hill is affected by various changes which have direct analogues in violin-making practice. First, parameters relating to the bridge will be tested. Figure 13 shows the effect of varying the mass and stiffness of the bridge in such a way that the ratio, and hence the clamped resonance frequency, is kept constant. The behaviour is as anticipated from eq. (19): the main effect is that the damping factor of the hill resonance varies over a wide range with relatively small changes in the mass and stiffness. The peak frequency of the hill remains close to the clamped frequency throughout: for these particular parameter values, as seen in Fig. 11, the reactive component of R_∞ is small in the relevant frequency range. From the perspective of a violin maker, this figure shows the effect of adjusting the bridge by thinning the entire structure: the mass and the stiffness will both vary in proportion to the thickness, and the ratio will remain constant. Such adjustment seems to give a very direct way to change the height and bandwidth of the bridge hill.

Figures 14 and 15 show the effect of varying the bridge-top mass keeping the stiffness constant, and conversely varying the stiffness keeping the mass constant. Both correspond to realistic bridge adjustment procedures: the mass is determined by the thickness of the top portion of the bridge (and by the bridge height and choice of wood), while the stiffness can be varied independently by trimming around the cutouts. In addition, Fig. 14 illustrates the effect of adding a mute to the violin bridge: the range of masses explored is sufficiently wide to cover variations of bridge shaping and typical mutes. As anticipated, both figures show a combination of varying hill frequency and bandwidth. Taken in combination with Figure 11, it would appear that by judicious bridge adjustment the hill frequency and bandwidth could both be placed wherever required on this simplified violin body. On a violin in which R_∞ showed a bigger reactive component there might be limits on the range over which the frequency and bandwidth could be adjusted (as shown by Jansson's test with the plate bridge [6]).

Finally, Jansson has shown an interesting series of measurements using bridges with different foot spacings d [7]. This experiment is simulated, approximately, in Fig. 16. Results are seen which qualitatively mirror the experimental findings. Decreasing the foot spacing reduces the peak frequency of the hill, by changing R_∞. Interestingly, for this model at least, the hill bandwidth varies at the same time in a non-obvious way. As the foot spacing is reduced from its normal value, the bandwidth increases to a maximum with a foot spacing around 20 mm, then decreases again when the spacing is reduced further. Note that the clamped bridge resonance remains at 3 kHz throughout this series of simulations, so that the shift in hill frequency is entirely due to changes in the reactive component of R_∞.

4.2. Parameters of the violin body

In a similar way, the model can be used to explore changes in the parameters of the violin body, keeping the bridge unchanged. Figures 17 and 18 show the influence of the thickness of the top and back plates respectively. The set of thicknesses tested were the same in both cases, 2–4 mm: in reality, a violin top plate would usually have a thickness in the bridge region towards the lower end of this range [16], while the back plate near the soundpost position would have a thickness at the upper end of the range. The results show similar tends in both cases, but not surprisingly the hill is affected much more sensitively by the top thickness than by the back thickness. A thinner top, and to a lesser extent a thinner back, has the effect of reducing the hill frequency and increasing its bandwidth. It also has a significant effect on the level of the skeleton curve at low frequencies, but it is an open question whether this aspect of the results carries over to a real violin body with its arched plates, since the frequencies in question are low enough that one would expect curvature to matter.

Finally, in Fig. 19 the effect of soundpost position is explored. The soundpost is moved along a line behind the "treble" foot of the bridge, parallel to the grain of the top plate. The distance between bridge foot and soundpost is varied in the range 5–30 mm. Ordinarily, the soundpost position would be near the lower end of this range. The results show only a rather slight influence on the bridge hill, one which could easily be compensated by small adjustments to the bridge. The well-known sensitivity of the sound of a violin to the position of the soundpost does not seem to be associated to any great degree with changes to the bridge hill, at least within this simplified model.

5. Conclusions and implications for violin makers

It has been shown that Reinicke's model for the deformation of a violin bridge in its lowest in-plane resonance [1,2] can be combined with a very simple model of violin body vibration to give a system which can elucidate the various published measurements relating to the bridge hill in the input admittance of a violin [6,7,8]. By replacing the finite plates in the body model by infinite plates, the calculation can directly yield the "skeleton" curve which underlies the bridge hill. Using the skeleton curve, the frequency and bandwidth of the hill were shown to vary in a simple and predictable way with the parameters which determine the behaviour of the bridge and the violin body model. There is obvious scope for experiments to test the predictions of this study by making controlled adjustments to bridges and measuring the effect on the input admittance and the bridge hill.

The results of this study are of direct interest to violin makers. The bridge model, and the formula (19) for the effective loss factor of the hill, is quite robust. Although the body model used here was highly schematic, the general conclusions about the effect of bridge adjustment on the frequency, height and bandwidth of the hill should carry over directly to the behaviour of a bridge on a real violin. If a "normal" bridge hill is desired (and one should not forget that the evidence for the significance of the hill comes only from correlation studies, not from psychoacoustical tests), then it should *always* be possible to create one on any reasonably conventional violin by suitable bridge adjustment.

Some instruments place constraints on the potential for shaping the hill by bridge adjustment, because the reactive contribution from the moment admittance of the body (R_∞) has a strong effect. Jansson's test instrument seems to be like this, because it showed a fairly normal hill even with the plate bridge with no cutouts [6]. But Dünnwald's data for "master instruments" (see Fig. 3 of ref. [3]) suggests that many high-quality instruments are not like this: his plot extends up to 7 kHz with little obvious sign of the low-pass filtering effect of the bridge hill, which should be present even when the hill loss factor exceeds unity so that there is no "hill" as such. It seems likely from the present study that these instruments could all be modified by adjusting their bridges, so that they behaved more like his set of "old Italian violins" (see the same figure [3]).

If a scientific approach to bridge adjustment were wanted, a possible procedure would be to start by measuring the input admittance of the violin in question using a Jansson plate bridge in order to calibrate the body behaviour. This would reveal the constraints imposed by the body behaviour, then it should be possible to adjust a bridge to bring the hill resonance to the right frequency range. At the same time the maker should be careful to monitor the bridge mass, to control the height and bandwidth of the hill. Note that the bridge height and foot spacing also have an influence, although in practice there is only limited scope to vary these. Another possible procedure might be to measure directly the 2×2 admittance matrix that describes the properties of the violin body at the two foot positions, then calculate the moment admittance R from eq. (3) and use it to optimise a "virtual bridge design" by computer. The real bridge could then be cut while making regular comparisons with the computer model to guide the adjustment process.

To understand why some violins seem to have a greater reactive component of R_∞ than others would require an extension of the modelling of the violin body. The idea of obtaining the skeleton curve by allowing the top and back plates to become infinite is still valid, but certain details of the violin structure are sufficiently close to the bridge that they should be included. The arching and graduation pattern of both plates around the bridge/soundpost area, the central portion of the bass bar and the free edges at the f-holes are all strong candidates for inclusion [8]. However, the more remote regions of the plates could be allowed to extend to infinity in some suitable way, perhaps by using absorbing boundaries in the computation so that no reflections were generated. If such a model could be analysed, probably using finite-element methods, it would allow the parameter study of section 4 to be extended to other aspects of the violin structure. Such a model may be a worthwhile subject of future research.

Acknowledgements

The author is grateful to Erik Jansson, Claire Barlow and Robin Langley for useful discussions on this work, to Martin Woodhouse for helping prepare Figure 1 and to Huw Richards for the violin whose response is shown in Fig. 2.

References

[1] L. Cremer: The Physics of the Violin, MIT Press, Cambridge MA 1985. See chapter 9.
[2] W. Reinicke: Die Übertragungseigenschaften des Streichinstrumentenstegs. Doctoral dissertation, Technical University of Berlin, 1973.
[3] H. Dünnwald: Deduction of objective quality parameters on old and new violins. J. Catgut Acoust. Soc. Series 2, 1, **7** (1991)1–5.
[4] E. V. Jansson: Admittance measurements of 25 high quality violins. Acustica – Acta Acustica **83** (1997) 337–341.
[5] E. V. Jansson, B. K. Niewczyk: Admittance measurements of violins with high arching. Acustica - Acta Acustica **83** (1997) 571–574.
[6] E. V. Jansson, B. K. Niewczyk: On the acoustics of the violin: bridge or body hill. J. Catgut Acoust. Soc. Series 2, 3, **7** (1999) 23-27.
[7] E. V. Jansson: Violin frequency response — bridge mobility and bridge feet distance. Submitted to Applied Acoustics (2004).
[8] F. Durup, E. V. Jansson: The quest of the violin bridge hill. Submitted to Acustica – Acta Acustica(2004).
[9] I. P. Beldie: About the bridge hill mystery. J. Catgut Acoust. Soc. Series 2, 4, **8** (2003) 9–13.
[10] C. H. Hodges, J. Woodhouse: Theories of noise and vibration transmission in complex structures. Reports on Progress in Physics **49** (1986) 107-170.
[11] M. E. McIntyre, J. Woodhouse: On measuring the elastic and damping constants of orthotropic sheet materials. Acta Metallurgica **36** (1988)1397–1416.
[12] E. Szechenyi: Modal densities and radiation efficiencies of unstiffened cylinders using statistical methods. J. Sound Vib. **19** (1971) 65–81.
[13] E. Skudrzyk: The mean-value method of predicting the dynamic response of complex vibrators. J. Acoust. Soc. Amer. **67** (1980) 1105–1135.
[14] R. Ohayon, C. Soize: Structural Acoustics and Vibration, Academic Press, San Diego CA, 1998. See chapter 15.
[15] L. Cremer, M. Heckl, E. E. Ungar: Structure-borne Sound, Springer, Heidelberg 1988. See section IV, 3d.
[16] J. S. Loen: Reverse graduation in fine Cremonese violins. J. Catgut Acoust. Soc. Series 2, 4, **7** (2003) 27-39.

Table 1. Standard parameter values for the "violin" and "bridge" models. Wood properties are typical of published data, except that no data are available for D_2 and D_4 for maple and these values have been guessed. Calculations of "skeleton" curves assume eq. (14), and thus disregard the values of D_2 and D_4 given here.

Plate property	Symbol	Unit	Spruce value	Maple value
Density	ρ	kg m^{-3}	420	650
Elastic constants	D_1	MPa	1100	860
	D_2	MPa	67	140
	D_3	MPa	84	170
	D_4	MPa	230	230
Length	L_1	mm	321	321
Width	L_2	mm	204	204
Thickness	h	mm	2.9	4.0

Property	Symbol	Unit	Value
Bridge foot positions	(x_1, y_1)	mm	(120,87)
	(x_2, y_2)	mm	(120,117)
Soundpost position	(x_3, y_3)	mm	(110,117)
Clamped frequency	$\Omega_b / 2\pi$	Hz	3000
Bridge mass	m	g	0.5
Bridge height	a	mm	20
Foot spacing	d	mm	30

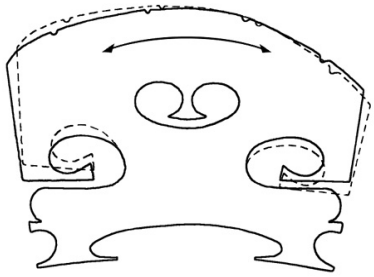

Figure 1. A violin bridge with an indication of the motion in the lowest in-plane bridge resonance.

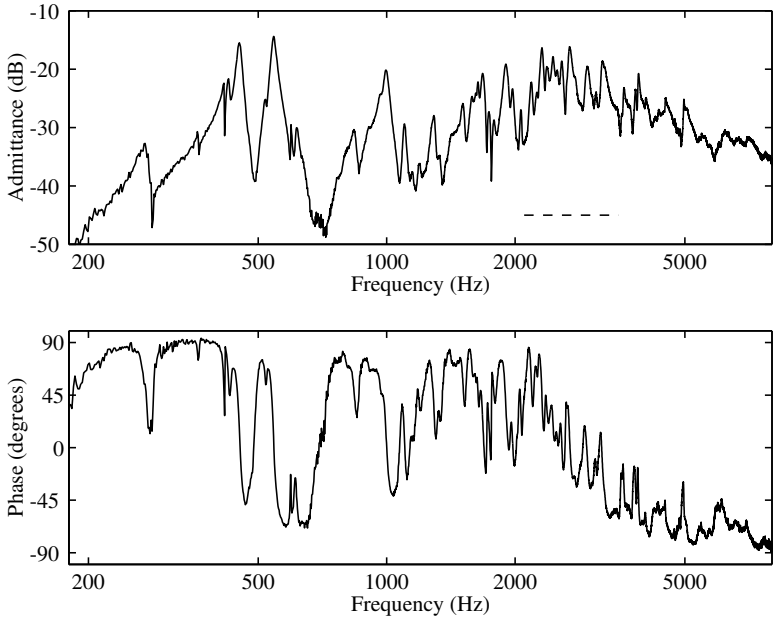

Figure 2. Input admittance of a violin, showing a typical bridge hill (in the frequency range indicated by the dashed line in the upper plot). The upper plot shows the magnitude in dB re $1\,\mathrm{m\,s^{-1}N^{-1}}$.

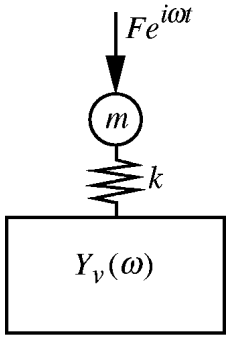

Figure 3. Sketch of a generic system driven through a resonator, as described in the text.

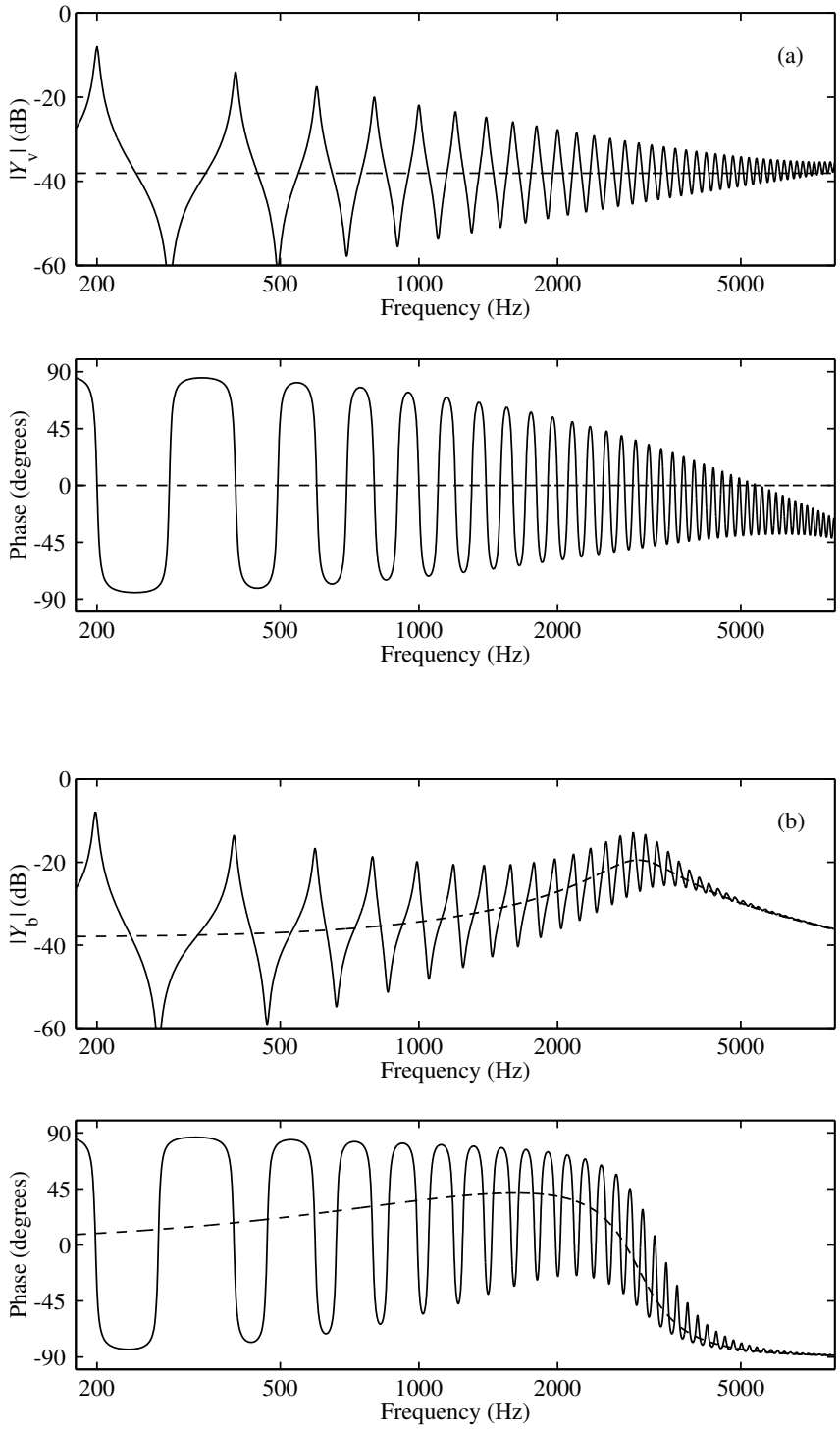

Figure 4. Frequency responses of an idealised system based on Fig. 3: (a) input admittance of the base system; (b) input admittance at the position of forcing, including the effect of the series oscillator and showing "bridge hill" behaviour. Dashed lines indicate the "infinite system" response skeleton as explained in section 3. The "body" has modes equally spaced at 200 Hz intervals, all with modal mass 0.1 kg and Q-factor 50. The "bridge" has mass 1.5 g and clamped frequency 3 kHz.

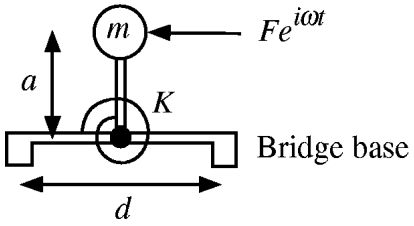

Figure 5. Idealised model of a violin bridge, including a single resonance to model the deformation shown in Fig. 1.

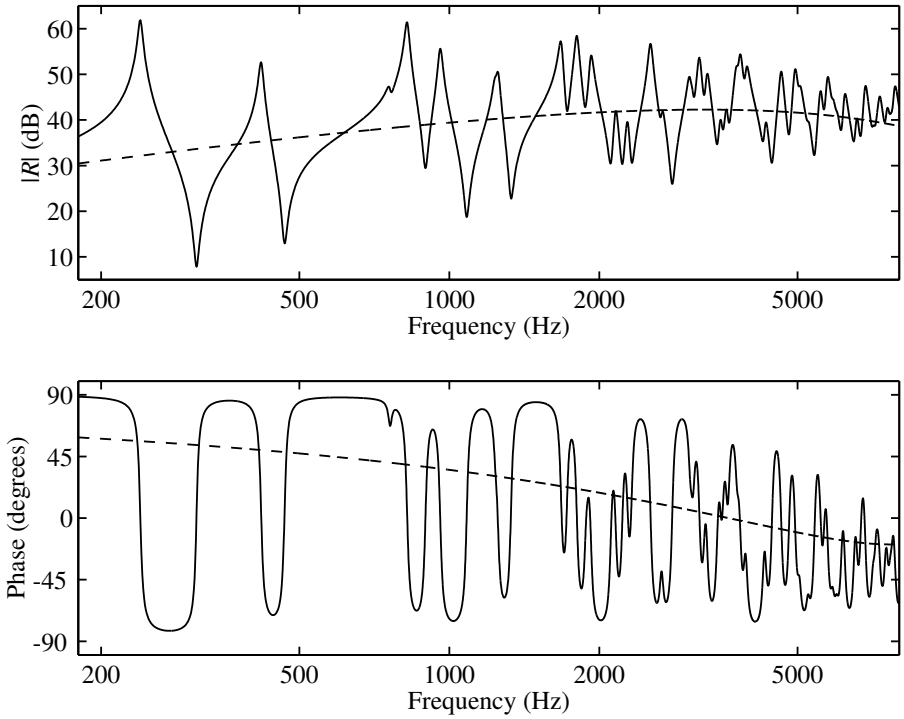

Figure 6. Rotational input admittance $R(\omega)$ of a rectangular spruce plate driven through the rigid "bridge base" of Fig. 5. Parameter values are given in Table 1. Dashed lines indicate the "infinite system" response skeleton $R_\infty(\omega)$ as explained in section 3.

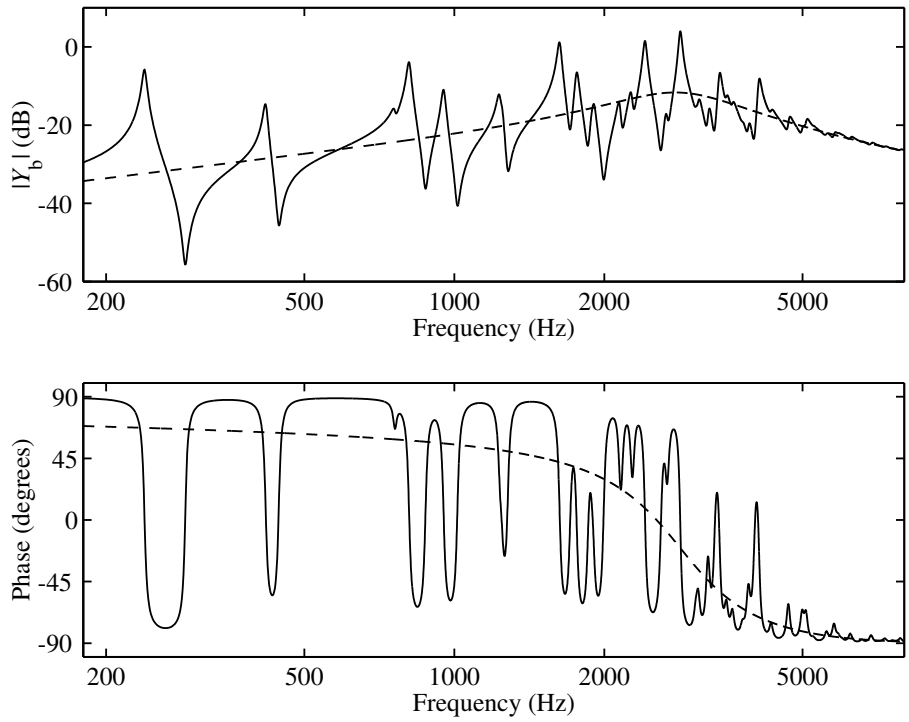

Figure 7. Input admittance of the plate system of Fig. 6 driven through the bridge model of Fig. 5. Parameter values are given in Table 1. Dashed lines indicate the "infinite system" response skeleton as explained in section 3.

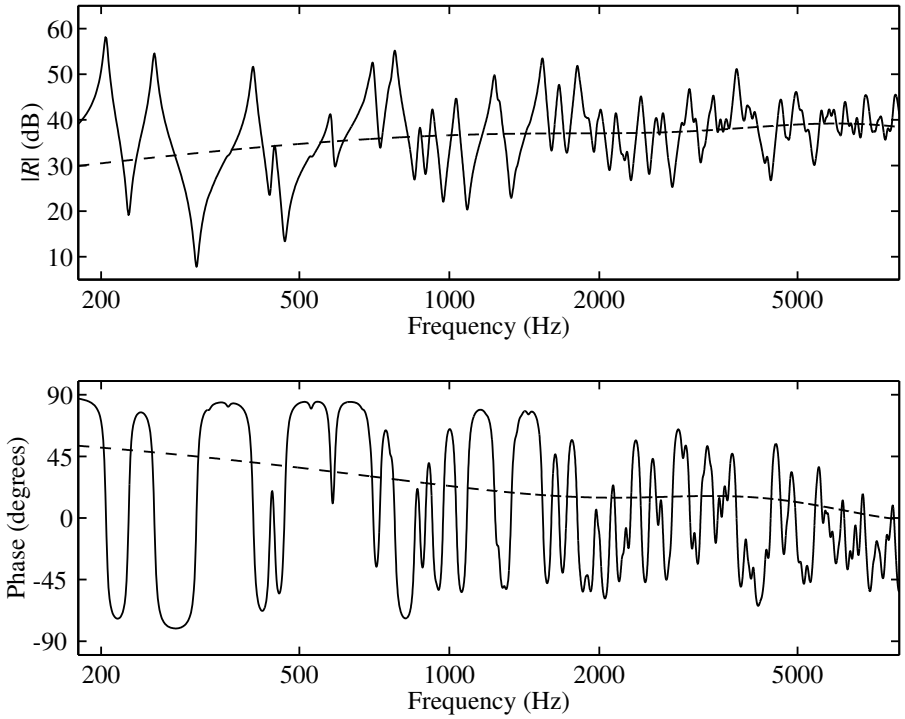

Figure 8. Rotational input admittance $R(\omega)$ of the "violin body" model described in the text, driven through the rigid "bridge base" of Fig. 5. Parameter values are given in Table 1. Dashed lines indicate the "infinite system" response skeleton $R_\infty(\omega)$ as explained in section 3.

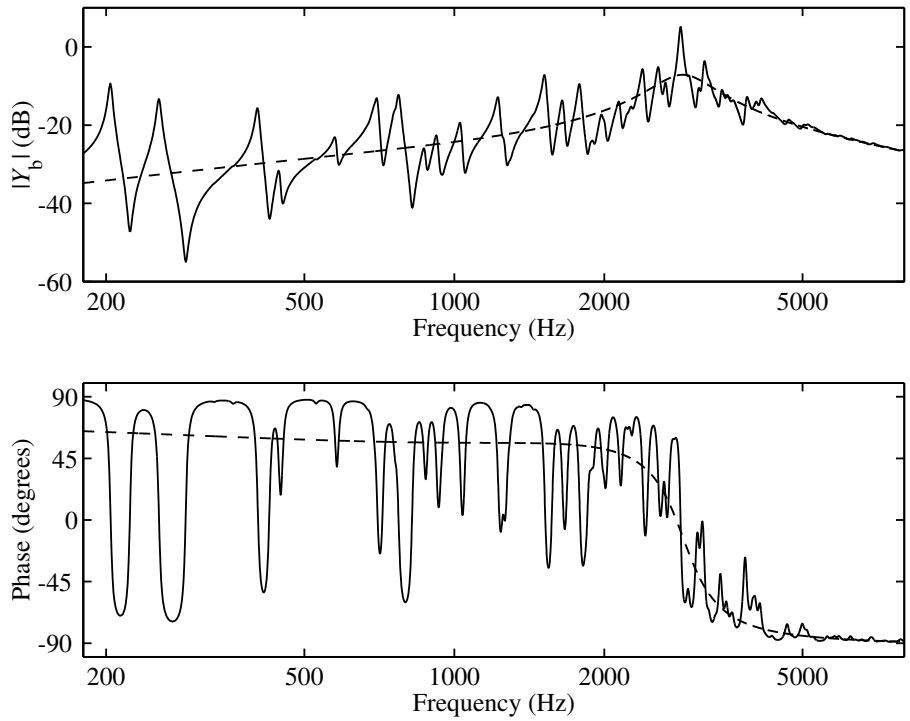

Figure 9. Input admittance of the "violin body" model of Fig. 8 driven through the bridge model of Fig. 5. Parameter values are given in Table 1. Dashed lines indicate the "infinite system" response skeleton as explained in section 3.

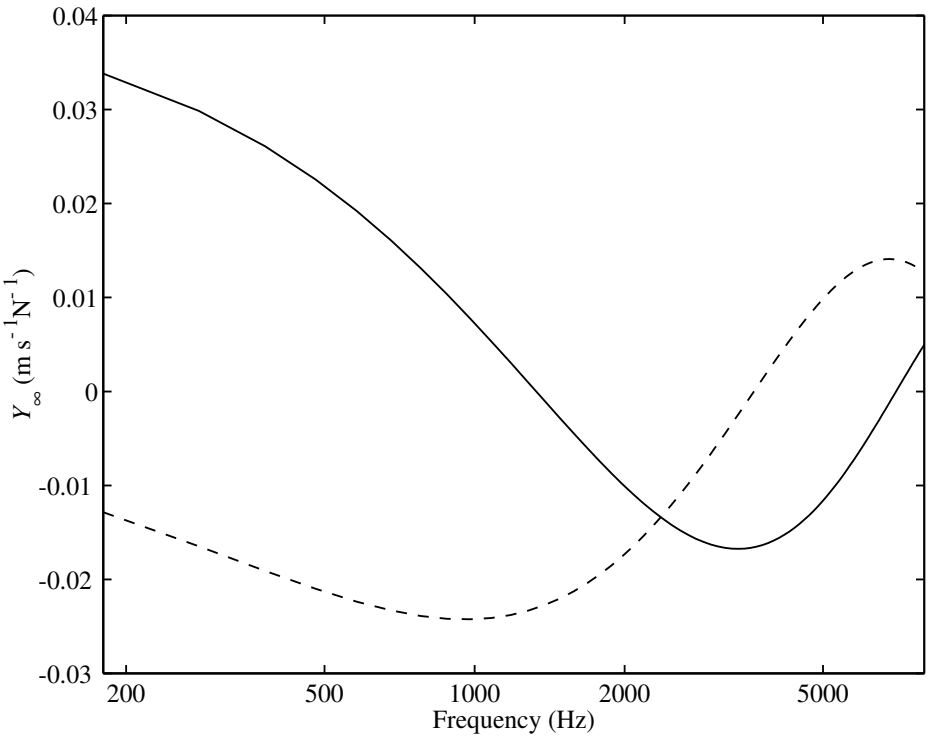

Figure 10. Real part (solid line) and imaginary part (dashed line) of the infinite-plate response from eq. (16) using parameter values from Table 1 and a distance *r* equal to the bridge foot spacing, 30 mm.

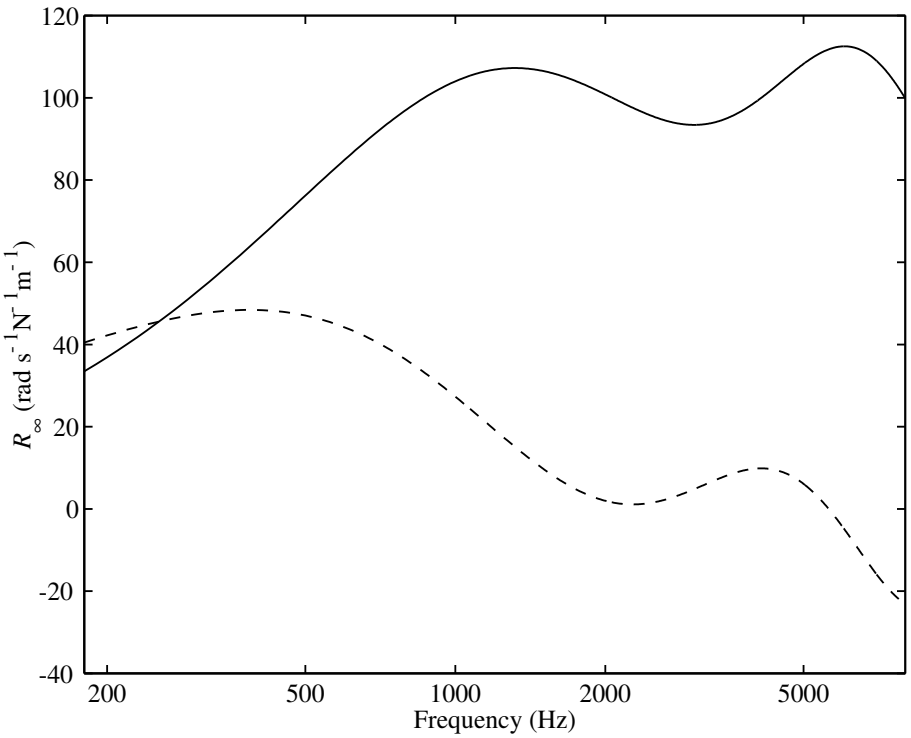

Figure 11. Real part (solid line) and imaginary part (dashed line) of the rotational input admittance $R_\infty(\omega)$ of the "skeleton" model described in the text. Parameter values are given in Table 1.

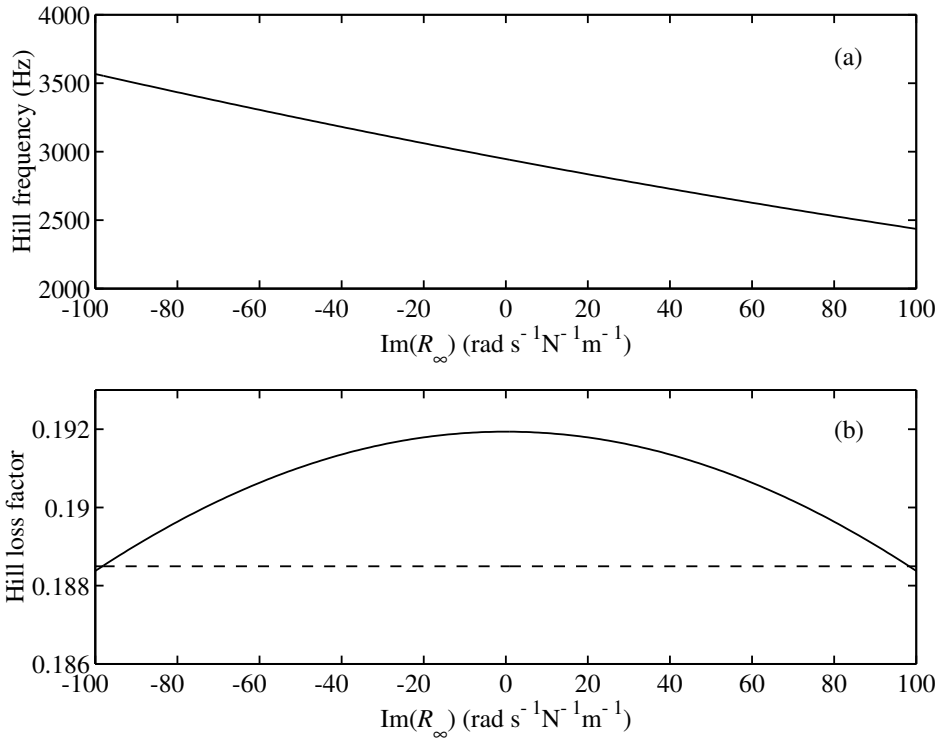

Figure 12. Variation of the "hill peak" properties from Eq. (18) with the imaginary part (assumed independent of frequency) of the skeleton rotational input admittance R_∞. The real part of R_∞ has the constant value 100 rad m^{-1}s^{-1}N^{-1}. Plot (a) shows the frequency given by $\mathrm{Re}(\omega)$; plot (b) shows the loss factor $\zeta_b = \mathrm{Im}(\omega) / \mathrm{Re}(\omega)$.

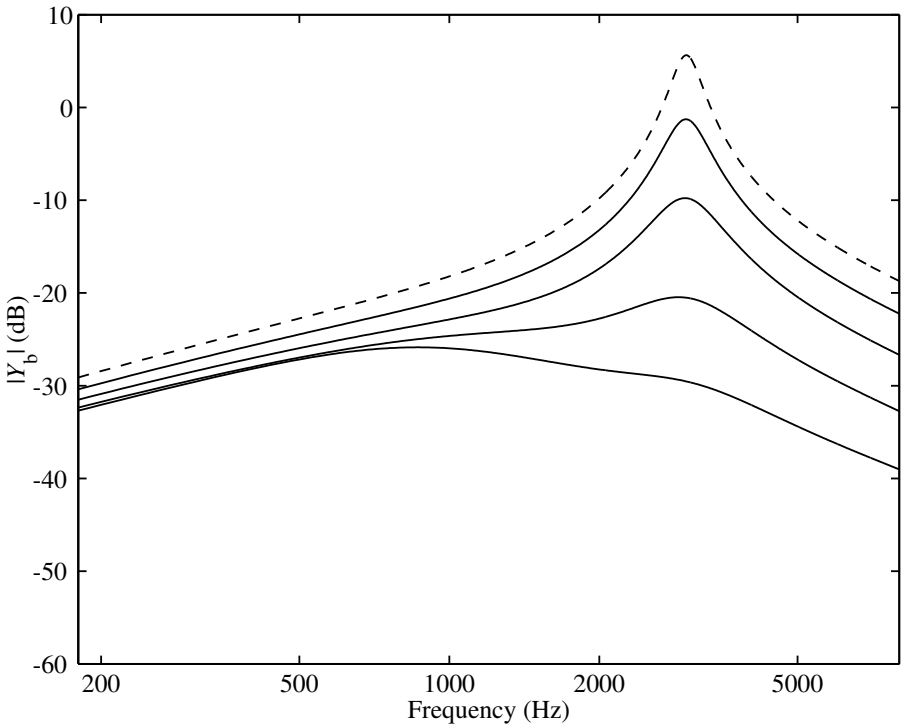

Figure 13. Skeleton curves for the input admittance showing variation of the bridge hill. Parameter values are as given in Table 1, except that the bridge mass and stiffness are varied while keeping the bridge frequency Ω_b fixed. The curves show mass m = 0.2, 0.3, 0.5, 1.0, 2.0 g, the first of these values being indicated by a dashed line and the others following in an obvious sequence.

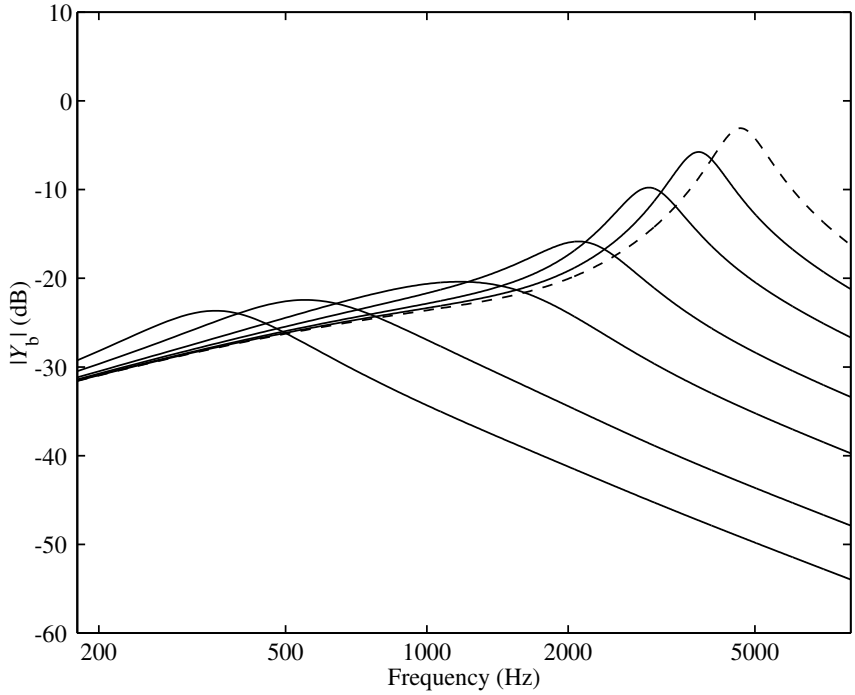

Figure 14. Skeleton curves for the input admittance showing variation of the bridge hill. Parameter values are as given in Table 1, except that the bridge mass is varied while keeping the bridge stiffness K fixed. The curves show mass m = 0.2, 0.3, 0.5, 1.0, 2.0, 5.0, 10.0 g, the first of these values being indicated by a dashed line and the others following in an obvious sequence. The lighter masses are intended to represent variations of bridge adjustment, while the heavier ones represent the effect of adding a mute.

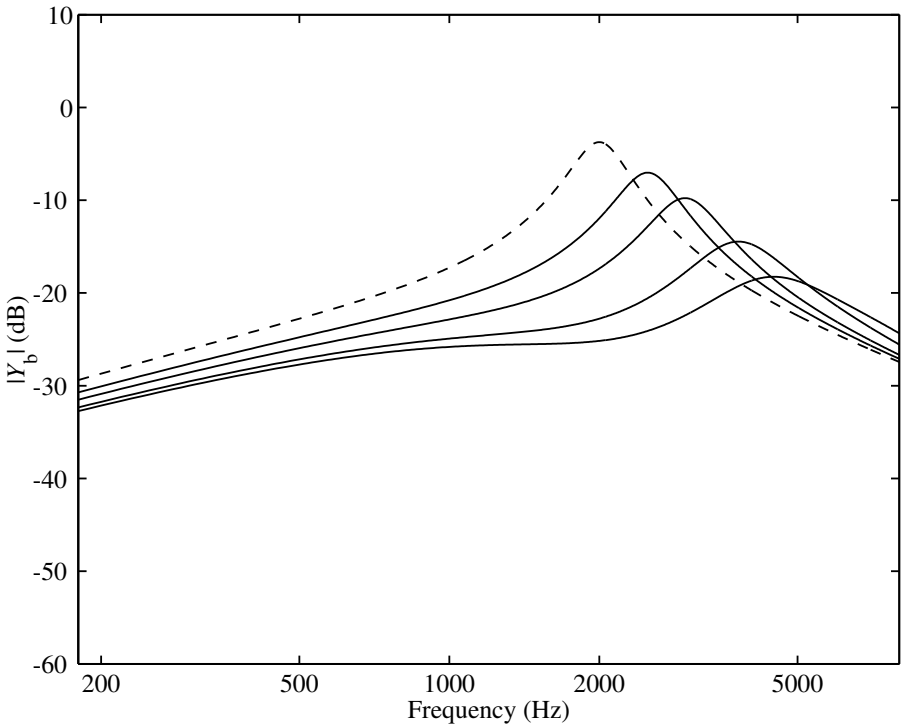

Figure 15. Skeleton curves for the input admittance showing variation of the bridge hill. Parameter values are as given in Table 1, except that the bridge stiffness K is varied while keeping the bridge mass m fixed. The curves are most conveniently indexed by the bridge frequency $\Omega_b / 2\pi$, which takes the values 2.0, 2.5, 3.0, 4.0, 5.0 kHz, the first of these values being indicated by a dashed line and the others following in an obvious sequence.

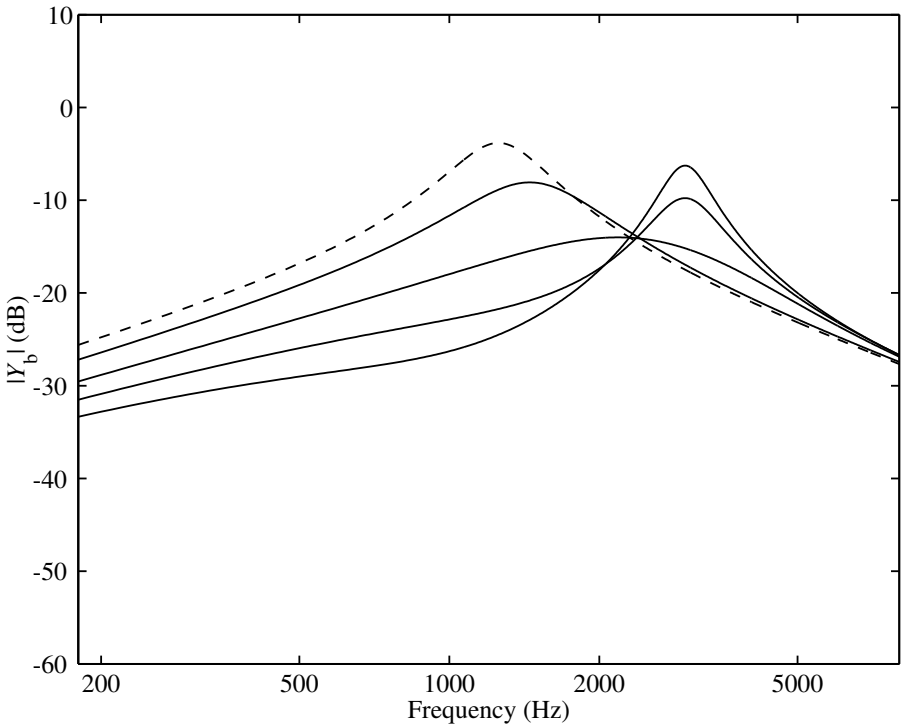

Figure 16. Skeleton curves for the input admittance showing variation of the bridge hill. Parameter values are as given in Table 1, except that the bridge foot spacing d is varied. The curves show d = 5, 10, 20, 30, 40 mm, the first of these values being indicated by a dashed line and the others following in an obvious sequence.

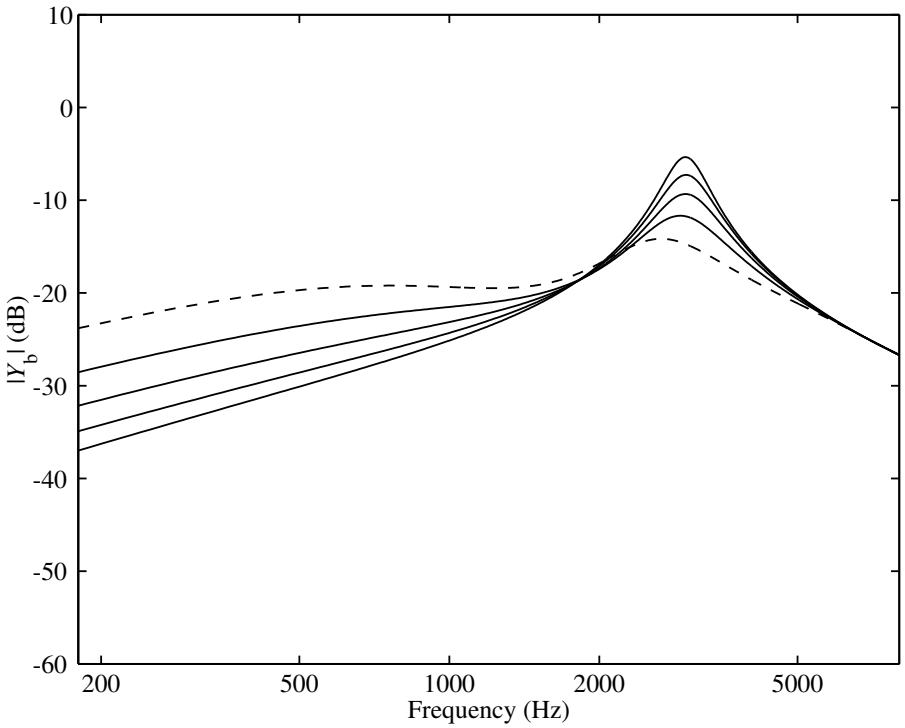

Figure 17. Skeleton curves for the input admittance showing variation of the bridge hill. Parameter values are as given in Table 1, except that the thickness of the spruce top plate is varied. The curves show thickness h = 2.0, 2.5, 3.0, 3.5, 4.0 mm, the first of these values being indicated by a dashed line and the others following in an obvious sequence.

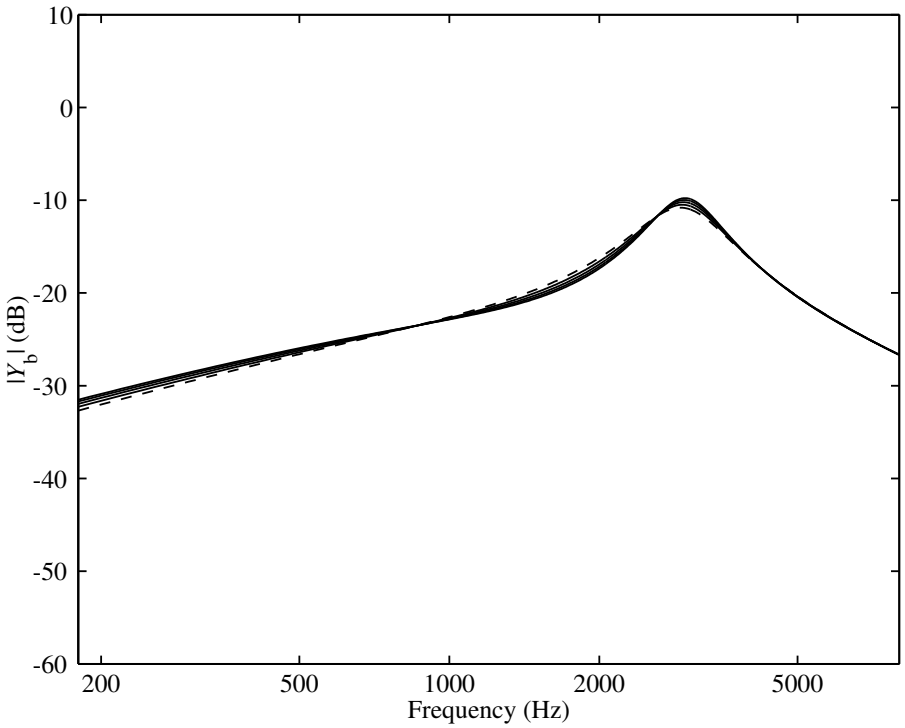

Figure 18. Skeleton curves for the input admittance showing variation of the bridge hill. Parameter values are as given in Table 1, except that the thickness of the maple back plate is varied. The curves show thickness h = 2.0, 2.5, 3.0, 3.5, 4.0 mm, the first of these values being indicated by a dashed line and the others following in an obvious sequence.

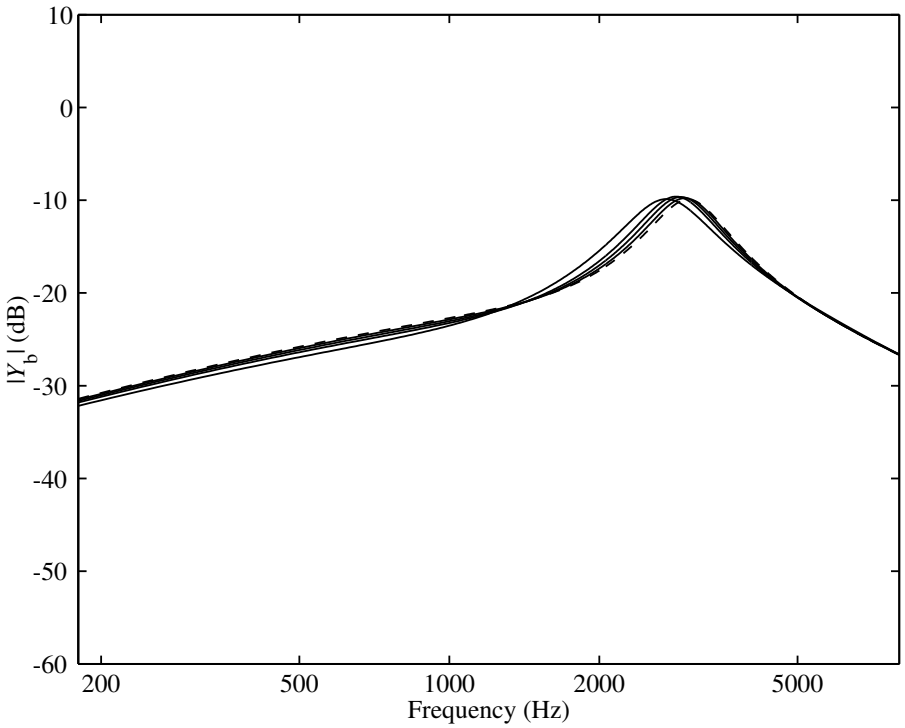

Figure 19. Skeleton curves for the input admittance showing variation of the bridge hill. Parameter values are as given in Table 1, except that the position x_3 ("parallel to the grain") of the soundpost is varied. The curves show soundpost offset $x_2 - x_3$ = 5, 10, 15, 20, 30 mm, the first of these values being indicated by a dashed line and the others following in an obvious sequence.